hep-ph/0609252
HRI-P-06-09-001
DO-TH 06/09
CU-PHYSICS-15/2006

Probing Lepton Number Violating Interactions with Beta-beams

Sanjib Kumar Agarwalla[a†], Subhendu Rakshit[b‡] and Amitava Raychaudhuri[†]

[†] *Harish-Chandra Research Institute, Chhatnag Road, Jhunsi, Allahabad - 211 019, India and Department of Physics, University of Calcutta, Kolkata - 700 009, India*

[‡] *Universität Dortmund, Institut für Physik, D-44221 Dortmund, Germany*

ABSTRACT

We show that a detector placed near a beta-beam storage ring can probe lepton number violating interactions, as predicted by supersymmetric theories with R-parity non-conservation. In the presence of such interactions, ν_τ can be produced during β-decay leading to tau leptons through weak interactions. Alternatively, electron neutrinos from β-decay of radioactive ions can produce tau leptons in a nearby detector through these interactions. The muons from the decay of these tau leptons can be readily identified in a small iron calorimeter detector and will signal violation of R-parity.

[a] E-mail address: sanjib@mri.ernet.in
[b] E-mail address: rakshit@zylon.physik.uni-dortmund.de

I Introduction

In the standard model (SM), lepton number (L) conservation is only accidental; the particle content and the requirement of renormalizability ensure that each lepton flavour number is conserved separately. However, non-zero neutrino masses, as indicated by recent neutrino oscillation experiments, have proved that the success of the SM should be viewed as that of a low energy effective theory. It is not unreasonable to expect that in some extensions of the SM, L conservation may not hold. Indeed, a Majorana mass term for the neutrinos violates total lepton number. The non-observation of direct L violation in the past experiments have put stringent constraints on some of these interactions. In this letter we show that beta-beams [1, 2, 3, 4, 5, 6, 7] and a nearby detector can be a good further probe of such interactions.

A beta-beam consists of a high intensity collimated beam of electron neutrinos produced from the beta decay of boosted radioactive ions. The recent progress in nuclear physics experimental techniques allows the design of beta-beams of high luminosity so that it can have comparable physics potential as that of proposed super-beam upgrades or even neutrino factories, which are technologically challenging at present. These beams may have widespread applications in particle physics, nuclear physics and astrophysics. The high collimation achievable with these beams allows neutrino oscillation experiments with long baselines[1]. However, for other physics studies, a small detector placed close to the source has been proposed. For this work, the advantage of a 'near' detector is twofold. Firstly, due to the short base-length, neutrinos do not get much scope to oscillate before being detected, which could otherwise mimic signals of the L-violating interactions ($\not{L}$). The other obvious advantage is that a larger part of the beam can be picked up with a smaller detector.

We consider placing a 5 kT cylindrical detector, aligned with the beam axis, within 1 km from the beta-beam storage ring. The L-violating interactions can lead to tau leptons in near-detector experiments in two ways. A ν_τ can be produced due to such interactions during β-decay, yielding a τ through weak charged current interactions in the detector. Alternatively, the electron neutrinos in the beam, produced through usual β-decay, can undergo L-violating interactions with the detector, leading to tau leptons. The taus promptly decay, part of the time in a muonic channel. Iron calorimeters with active detector elements serve well for identifying these muons, which leave long tracks in the detector, and for filtering out backgrounds. We will also briefly comment on water Čerenkov and other detectors.

In the following section we present a brief account of the experimental setup. In section III, $\not{L}$ interactions are discussed in the context of R-parity violating (RPV) supersymmetry [8, 9]. We stress how β-decay can be affected in the presence of such interactions, yielding ν_τ in a few cases in place of the standard ν_e. We also describe the processes via which ν_e produce tau leptons in the detector. The expected number of muon events from tau decay and the

[1] In [5] it was pointed out that these beams while traversing a long base-length can get influenced by L-violating interactions through matter effects, thus polluting oscillation signals.

Ion	$t_{1/2}$ (s)	E_0 (MeV)	f	Decay fraction	Beam
$^{18}_{10}$Ne	1.67	3.41	820.4	92.1%	ν_e
$^{6}_{2}$He	0.81	3.51	934.5	100%	$\bar{\nu}_e$
$^{8}_{5}$B	0.77	13.92	600684.3	100%	ν_e
$^{8}_{3}$Li	0.83	12.96	425355.2	100%	$\bar{\nu}_e$

Table 1: *Half-life, end-point energy E_0, f-value and decay fraction for various ions proposed for beta-beams [14]. In the presence of RPV couplings, β-decay of these ions can give rise to neutrinos and anti-neutrinos of other flavours with tiny branching ratios.*

constraints ensuing in the event of their non-observation will be presented in section IV.

II Beta-beam flux at a near-detector

The proposal of a beta-beam was put forward by Zucchelli [1]. It is based on the concept of creating a pure, intense, collimated beam of ν_e or $\bar{\nu}_e$ through the beta decay of completely ionized radioactive ions. It will be achieved by producing, collecting, and accelerating these ions and then storing them in a ring. This proposal is being studied in depth and will take full advantage of the existing CERN accelerator complex. The main future challenge lies in building an intense proton driver and the hippodrome-shaped decay ring which are essential for this programme.

For generating the ν and $\bar{\nu}$ beams, the commonly examined ions are ^{18}Ne and ^{6}He, respectively [10]. The beams are almost free from all types of *systematics*. The energy reach of these beta-beams depend on the relativistic boost factor γ. Using the existing CERN-SPS accelerator up to its maximum power, it will be possible to achieve $\gamma \sim 250$ [11]. A medium $\gamma \sim 500$ beta-beam would require a refurbished SPS with superconducting magnets or an acceleration technique utilizing the LHC [3, 11, 12]. A high $\gamma \sim 800$ could be achievable in the LHC era [13].

The choice of ions for a beta-beam is predicated by the intended physics. The low end-point energies (cf. Table 1) of the ^{6}He and ^{18}Ne ions restrict the energy reach of the beam; a threshold energy of 3.5 GeV is necessary to produce a τ-lepton from an incoming neutrino. Therefore, we choose to consider the recent proposal [15] of replacing the ^{6}He and ^{18}Ne ions by ^{8}Li and ^{8}B ions respectively, offering higher end-point energies. This option holds promise as it has been shown [15] that intense ^{8}Li and ^{8}B fluxes can be obtained by the ionisation cooling technique. Higher E_0 implies that, for a given γ, the neutrino beams will be more efficient in producing tau leptons. ^{8}Li and ^{8}B possess similar half-life and A/Z ratio as ^{6}He and ^{18}Ne, respectively. So they share the same key characteristics for bunch manipulation [16]. We pick only the neutrino beam for our discussion.

The geometry of the beta-beam storage ring determines the neutrino flux at a near-detector. For a low-γ design, a 6880 m decay ring with straight sections of length ($\equiv S$) 2500 m each (36% useful length for ion decays) has been proposed. In such a configuration, $N_0 = 1.1\times10^{18}$ useful decays (decays in one of the straight sections) per year can be obtained with ^{18}Ne ions [17, 18]. We have used this same luminosity for ^{8}B and higher γ [19]. To settle these issues a dedicated study is on at CERN.

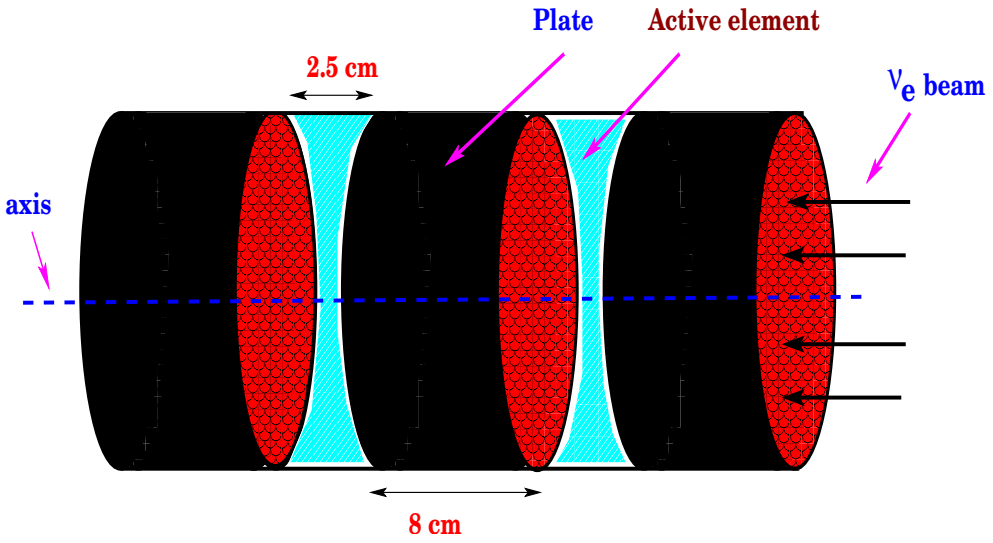

Figure 1: A schematic diagram of the proposed detector (a part only). The incoming ν_e beam may have a very small contamination of neutrinos of other flavours in the presence of lepton flavour violating interactions.

II.1 Detector Simulation Study

We consider a cylindrical 5 kT detector (as in Fig. 1) aligned with one of the straight sections of the storage ring. The detector is made of iron slabs (thickness 8 cm) with interleaved active detector elements (thickness 2.5 cm) such as resistive plate chambers (RPCs). The readouts from these RPCs will be concentric annular strips of small width with further segmentation to improve the position resolution. In this proposal, iron is the main content of the detector[2]. The thickness of the slabs ensures that electrons do not propagate in the detector. The signal muons are of sufficient energy to give rise to long tracks. To eliminate possible beam-induced backgrounds (see below) from pions produced in charged and neutral current processes, typically 6 to 13 hits (depending on the boost γ ranging from 250 to 450) are required of a putative muon track.

As noted earlier, the signature of new physics we consider is the appearance of prompt tau leptons which decay into muons with a branching fraction of 17.36% [20]. The tau produc-

[2]Lead may be an interesting alternative material to enhance the event rate.

tion threshold is around 3.5 GeV. This is what necessitates the higher boost γ.

Backgrounds, other than those of the beam-induced variety discussed below, are controllable, as we now point out. A beam-off run will help make a first estimate of these backgrounds. Further, an important aspect of the beta-beam source is its capability of eliminating backgrounds through timing information. The beam itself will consist of bunches of typically 10ns size and the number of bunches will be chosen so as to ensure that the ratio of the active- to the dead-time is $\mathcal{O}(10^{-3})$ [21]. Backgrounds from other sources, namely, atmospheric neutrinos, spallation neutrons, cosmic rays, etc. can thus be largely rejected from the time-stamp of a recorded event. Even further reductions of the backgrounds of external origin can be envisioned through fiducial and directionality cuts.

Now let us turn our attention to the issue of beam-induced backgrounds caused by neutral and charged current interactions of unoscillated ν_e. Electrons produced through weak interactions by the incoming ν_e are quickly absorbed and do not leave any track. Formation of prompt muons through R-parity violating supersymmetric interactions is suppressed by strong bounds on the relevant couplings arising from limits on $\mu - e$ transitions in atoms [22]. However, the beta-beam neutrinos can produce pions along with other hadrons at the detector via charged current and neutral current processes. They undergo strong interactions with the detector material and are quickly absorbed before they can decay. But as numerous pions are produced, it needs to be checked whether some of them can fake the signal.

We have checked our naïve expectations with a detector simulation study using GEANT [23] aided by NUANCE [24]. We observe that for neutrino-nucleon interactions at energies interesting for our study, the produced lepton preferentially carries most of the energy of the incident neutrino. Moreover, pions are usually produced with multiplicity more than unity. Hence it is not unreasonable to expect that the pions will be less energetic compared to the taus produced via $\not{L}$ interactions and hence in detectors of this genre, it is possible to distinguish hadronic showers from a muon track.

However, we followed a conservative approach in pion background estimation. Although pions do not leave behind a straight track like a muon, we still count the number of hits as a measure of the distance traversed by a pion. We impose a criterion of minimum number of hits to identify a track to be a muon one. We find from a simulation that, for $\gamma = 250/350/450$, imposing a cut of 6/10/13 hits will reduce the pion background at least to the 10^{-3} level.

The detector geometry plays a role in determining the signal efficiency after imposition of these cuts. Since the muons produced from boosted tau lepton decay carry transverse momentum, some of them may exit the detector through its sides, failing to satisfy the cuts. For a fixed detector mass (5 kT), a longer detector has a smaller cross-sectional area, resulting in a drop in the detector efficiency for the above reason. As the detector length increases from 20 m to 200 m, with our set of cuts, the efficiency factor reduces from 85%

to 70% approximately, showing little dependence on γ (see Fig. 2).

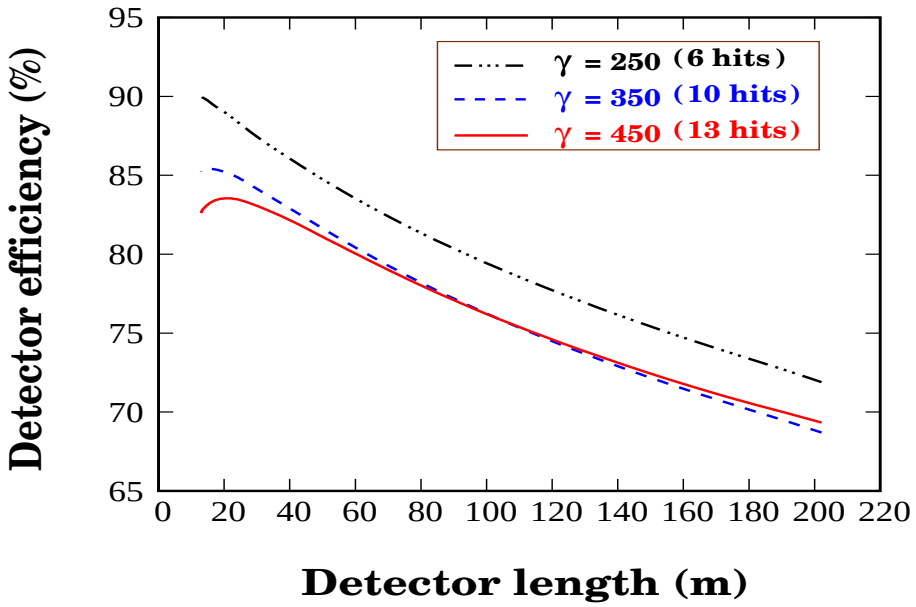

Figure 2: Detector efficiency for $\gamma = 250, 350, 450$. The corresponding cuts on muon hits used are 6, 10 and 13 respectively.

II.2 Neutrino fluxes

Neglecting small Coulomb interactions, the lab frame neutrino beta-beam flux (per unit solid angle per unit energy bin per unit time per unit length of the straight section) emitted at an angle θ with the beam axis is described by [4]

$$\phi(E_\nu, \theta) = \frac{1}{4\pi}\frac{g}{m_e^5 f}\frac{1}{\gamma(1-\beta\cos\theta)}\, E_e^\star\, (E_\nu^*)^2\, \sqrt{(E_e^\star)^2 - m_e^2} \tag{1}$$

where $E_e^\star (\equiv E_0 + m_e - E_\nu^*)$, and $E_\nu^* (\equiv E_\nu\gamma(1-\beta\cos\theta))$ are the rest frame energies of the emitted electron and the neutrino[3]. $g \equiv N_0/S$ is the number of useful decays per unit time per unit length of the straight section. m_e represents the electron mass. f and E_0 refer to the decaying ion as listed in Table 1.

To calculate the resulting number of events at a cylindrical near-detector of radius R and length D aligned with the beam axis it is necessary to integrate over the length S of the straight section of the storage ring and the volume of the detector. The event rate at a detector placed at a distance L from the storage ring is given by [25]

$$\frac{dN_{\not\ell}}{dt} = n\varepsilon \int_0^S dx \int_0^D d\ell \int_0^{\theta'} d\theta\, 2\pi \sin\theta \int_{E_\nu^{min}}^{E'_\nu} dE_\nu\, \phi(E_\nu, \theta)\, \sigma(E_\nu), \tag{2}$$

[3]Quantities without the '$*$' refer to the lab frame.

where

$$\tan\theta'(x,\ell) = \frac{R}{L+x+\ell} \quad \text{and} \quad E'_\nu = \frac{E_0}{\gamma(1-\beta\cos\theta)}. \tag{3}$$

Here n represents the number of target nucleons per unit detector volume, ε is the detector efficiency as presented in Fig. 2, E_ν^{min} denotes the tau production threshold, and $\sigma(E_\nu)$ stands for the neutrino-nucleon cross section. Note that the source of L-violation may lie either in $\phi(E_\nu,\theta)$ (in case of RPV β-decay) or in $\sigma(E_\nu)$ (in case of RPV tau production).

To help subsequent discussion, following [25], we rewrite the above formula isolating the geometry integrated total flux $\Phi(E_\nu; S, D, R, L)$ (per unit time per unit energy bin) falling on the detector and emitted from the whole length of the straight section as follows:

$$\frac{dN_{\not L}}{dt} = n\varepsilon \int_{E_\nu^{min}}^{E_\nu^{max}} dE_\nu \Phi(E_\nu; S, D, R, L)\, \sigma(E_\nu), \tag{4}$$

where

$$\Phi(E_\nu; S, D, R, L) = \int_0^S dx \int_0^D d\ell \int_0^{\theta'} d\theta\, 2\pi \sin\theta\, \phi(E_\nu,\theta) \tag{5}$$

and

$$E_\nu^{max} = \frac{E_0}{\gamma(1-\beta)}. \tag{6}$$

The beta-beam also involves a few small uncertainties which we neglect in our analysis. However for completeness, we list them here:

- There exist different excited states of the daughter nuclei of the decaying ion, which additionally lead to small contributions to the spectra with different endpoint energies.
- The ion beam has a finite transverse size. However, as this size varies [26] between only 3.0 cm to 5.1 cm, with an average of 4 cm (3σ), in both transverse directions inside the ring, the variation in flux at the detector due to this is negligible.
- The decaying ions may have small transverse momentum due to thermal fluctuations ($k_BT \sim 2.6\times10^{-3}$ eV), but this can be safely ignored in comparison with the end-point energy of the beta decay.

III L violating processes

Lepton number violation arises naturally as one supersymmetrises the standard model. In the minimal supersymmetric standard model, lepton number and baryon number (B) conservation is ensured by invoking 'R-parity'. It is a discrete Z_2 symmetry under which the SM particles are even and their superpartners are odd. The imposition of such a symmetry, while it serves a purpose, is rather *ad hoc*. In general, from the naïve theoretical point of view it is expected that L and B conservation does not hold in supersymmetric theories. However, as this leads to a very fast proton decay, we follow a common practice and assume

that B is conserved. This can be ensured by replacing the Z_2 symmetry of R-parity by a Z_3 symmetry, the so-called 'baryon triality' [27]. In such a scenario, in addition to the usual Yukawa interactions, the superpotential contains renormalizable L-violating trilinear λ- and λ'-type couplings and bilinear μ_i couplings:

$$W_{\not L} = \frac{1}{2}\lambda_{ijk} L_i L_j E^c_k + \lambda'_{ijk} L_i Q_j D^c_k + \mu_i L_i H_u, \tag{7}$$

where $i, j, k = 1, 2, 3$ are generation indices. Here L_i and Q_i are $SU(2)$-doublet lepton and quark superfields respectively; E_i, D_i denote the right-handed $SU(2)$-singlet charged lepton and down-type quark superfields respectively; H_u is the Higgs superfield which gives masses to up-type quarks. λ_{ijk} is antisymmetric under the interchange of the first two generation indices. The bilinear couplings, μ_i, are severely constrained by the small neutrino masses. So we will discuss the phenomenology of λ and λ' type couplings only. Then, the above superpotential leads to the following Lagrangian:

$$\begin{aligned}
\mathcal{L}_{\not L} &= \lambda'_{ijk} \,[\, \tilde{d}^j_L \, \bar{d}^k_R \nu^i_L + (\tilde{d}^k_R)^* (\bar{\nu}^i_L)^c d^j_L + \tilde{\nu}^i_L \bar{d}^k_R d^j_L \\
&\qquad - \tilde{e}^i_L \bar{d}^k_R u^j_L - \tilde{u}^j_L \, \bar{d}^k_R e^i_L - (\tilde{d}^k_R)^* (\bar{e}^i_L)^c u^j_L] \\
&\quad + \frac{1}{2}\lambda_{ijk} \,[\, \tilde{e}^j_L \, \bar{e}^k_R \nu^i_L + (\tilde{e}^k_R)^* (\bar{\nu}^i_L)^c e^j_L + \tilde{\nu}^i_L \bar{e}^k_R e^j_L - (i \leftrightarrow j)] + h.c.
\end{aligned} \tag{8}$$

The above interaction terms violate lepton number, L, as well as lepton flavour number. Suitable combinations of two such terms can lead to processes which are lepton flavour violating but L-conserving. The study of such non-standard interactions at a neutrino factory has been undertaken in [28, 29]. Influence of these interactions in the context of long baseline beta-beam experiments was studied in [5]. Here we examine the physics potential of beta-beams to explore such interactions in a near-detector scenario. To impose conservative upper bounds, we work in a minimal RPV framework where only a pair of such couplings are assumed to be non-zero at a time.

For a near-detector, RPV can come into effect in two ways as described in the following subsections.

III.1 RPV and ν_τ production in β-decay

RPV interactions can drive beta decay producing ν_τ instead of ν_e (see Fig. 3(a)). ν_τ so produced give rise to τ leptons in the detector which may decay in the leptonic channel producing muons.

Simultaneous presence of λ'_{31k} and λ'_{11k} couplings can be responsible for producing a ν_τ in β-decay. Of these, λ'_{111} is tightly constrained from neutrinoless double beta decay [30]. But the upper bound on the combination $|\lambda'^{\star}_{31k}\lambda'_{11k}|, k = 2, 3$ is rather relaxed; a limit of $2.4\times10^{-3}(\tilde{m}/100 \text{ GeV})^2$, $\tilde{m}$ being a common sfermion mass, follows from $\tau^- \to e^-\rho^0$ [22, 20]. $\tilde{m}$ denotes a common sfermion mass. The corresponding decay amplitude can be written as,

$$M_{\not L}(u \longrightarrow d e^+ \nu_\tau) = \frac{\lambda'^{\star}_{31k}\lambda'_{11k}}{2(\hat{s} - \tilde{m}^2)} \,[\bar{u}_{\nu_\tau}\gamma_\mu P_L u_e] \,[\bar{u}_d \gamma^\mu P_L u_u]. \tag{9}$$

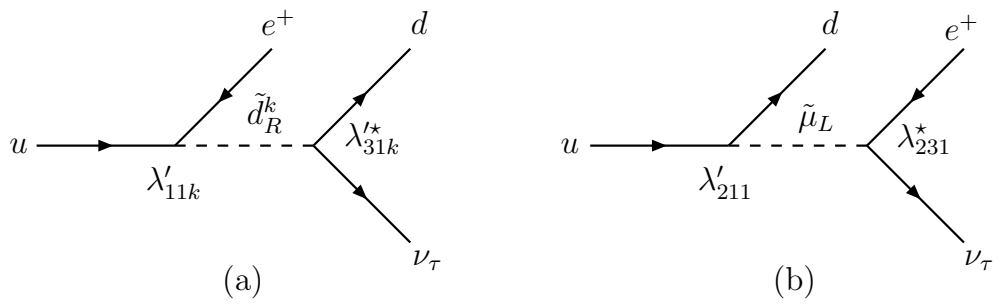

Figure 3: Feynman diagrams for RPV driven β-decay through (a) $\lambda'\lambda'$ and (b) $\lambda\lambda'$ type trilinear product couplings. Substantial event rates are obtained in (a) when $k = 2, 3$.

Alternatively, ν_τ can be produced in β-decay if another combination of RPV couplings $\lambda^{\star}_{i31}\lambda'_{i11}$ ($i = 1,2$) is non-zero (see Fig. 3(b)). As mentioned earlier, λ'_{111} is severely constrained. The combination $|\lambda^{\star}_{231}\lambda'_{211}|$ is bounded from above by $1.6 \times 10^{-3}(\tilde{m}/100\ \text{GeV})^2$ arising from the decay channel $\tau^- \to e^-\eta^0$ [22, 20], which is not too small to produce an observable effect. The corresponding decay amplitude is given by,

$$M_{\not L}(u \longrightarrow d e^+ \nu_\tau) \;=\; \frac{\lambda^{\star}_{231}\lambda'_{211}}{(\hat{t} - \tilde{m}^2)}\,[\bar{u}_{\nu_\tau} P_R\, u_e]\,[\bar{u}_d P_L u_u]. \tag{10}$$

III.2 RPV in tau production from ν_e

ν_e produced through ordinary β-decay driven by weak interactions can undergo RPV interactions with the detector producing τ which subsequently decay into muons.

Simultaneous presence of λ'_{31k} and λ'_{11k} couplings can give rise to τ^- in the final state from an incoming ν_e of the beta-beam (see Fig. 4(a)). The amplitude for the corresponding s-channel diagram can be written, after a Fierz transformation, as

$$M_{\not L}(\nu_e\, d \longrightarrow \tau^-\, u) \;=\; \frac{\lambda'^{\star}_{31k}\lambda'_{11k}}{2(\hat{s} - \tilde{m}^2)}\,[\bar{u}_\tau \gamma_\mu P_L u_{\nu_e}]\,[\bar{u}_u \gamma^\mu P_L u_d]. \tag{11}$$

An alternative channel of tau production from an incoming ν_e beam exists (see Fig. 4(b)) if a particular combination of the λ and λ' couplings $\lambda_{i13}\lambda'^{\star}_{i11}$ (i = 2,3) is non-zero. Here again, λ_{313} is severely constrained from neutrinoless double beta decay experiments [31]. An upper bound of $1.6 \times 10^{-3}(\tilde{m}/100\ \text{GeV})^2$ applies to the combination $|\lambda_{213}\lambda'^{\star}_{211}|$, from the decay channel $\tau^- \to e^-\eta^0$ [22, 20]. The amplitude for this t-channel process is

$$M_{\not L}(\nu_e\, d \longrightarrow \tau^-\, u) \;=\; \frac{\lambda_{213}\lambda'^{\star}_{211}}{(\hat{t} - \tilde{m}^2)}\,[\bar{u}_\tau P_L u_{\nu_e}]\,[\bar{u}_u P_R u_d]. \tag{12}$$

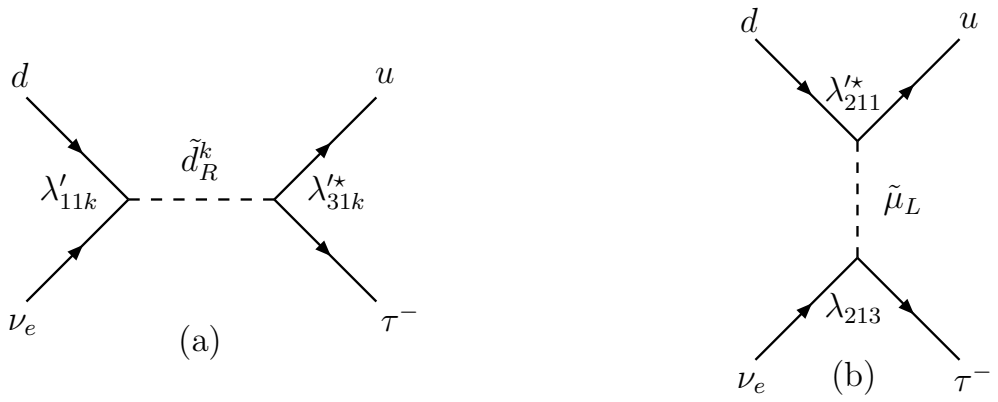

Figure 4: Feynman diagrams for tau production from an incoming ν_e beta-beam through (a) $\lambda'\lambda'$ and (b) $\lambda\lambda'$ type trilinear product couplings. Substantial event rates are obtained in (a) when $k = 2, 3$.

In what follows, we categorise the above two kinds of diagrams (a) and (b) in Figs. 2 and 3 as $\lambda'\lambda'$ and $\lambda\lambda'$ processes, respectively.

Note that, if $|\lambda'^{\star}_{31k}\lambda'_{11k}|, k = 2, 3$ is non-zero, tau leptons can be produced at the detector either due to RPV interactions affecting β-decay or due to RPV interactions of a ν_e with the detector material. These two equal contributions add in the total rate of tau production.

However, for the $\lambda\lambda'$ process, we see that the RPV combinations $|\lambda^{\star}_{231}\lambda'_{211}|$ (which drive the RPV beta decay) and $|\lambda_{213}\lambda'^{\star}_{211}|$ (which is responsible for producing a tau from an incoming ν_e in the detector) are different. As we are following the strategy of taking only two RPV couplings non-zero at a time, these contributions, which are of the same magnitude, cannot be present at the same time.

In passing, a few comments are in order:

- In both diagrams, the incoming ν_e can interact with a $\bar{u}$ quark from the sea to produce a tau. Due to the smallness of the corresponding parton distribution function, this contribution is suppressed but we do include it in the numerical evaluations.

- Here we should mention that the flavour changing neutral current process, $K^+ \to \pi^+\nu\bar{\nu}$ [32] puts stringent bounds on all the λ' couplings. However, these are basis dependent and hence can be evaded.

- As already noted, the non-observation of the process $\mu \to e(Ti)$ severely restricts [9, 22] the possibility of emitting a ν_μ in β-decay and direct production of muons from an incoming ν_e beam.

- Since the beta-beam energy is $\sim$ a few GeV, the expected event rate will be essentially independent of the sfermion mass as the bounds on λ, λ' scale with $(\tilde{m}/100\ \text{GeV})^2$.

At this energy range it is important to consider contributions from deep-inelastic, quasi-elastic, and single-pion production channels. To estimate the RPV deep-inelastic scattering cross section, we have used CTEQ4LQ parton distributions [33]. RPV quasi-elastic scattering and single-pion production cross sections have been evaluated from the corresponding SM cross sections[4] [34] by a rescaling of the couplings. We have noticed that, as eq. 12 is not reducible to an SM-like $(V-A)\otimes(V-A)$ Lorentz structure, in calculating DIS cross section a factor $\sim 1/3$ appears from polar integration compared to that for eq. 11. For the $\lambda\lambda'$ process we have adopted the same suppression factor for the SM quasi-elastic and single-pion production cross sections as well. Conservatively, we assume that a similar suppression also applies to the case of RPV β-decay. It bears stressing that the effect of the tau mass is felt on the neutrino-nucleus cross section throughout the energy range beyond the τ-threshold and this is included in the analysis.

IV Results

A near-detector setup is qualitatively different from a far-detector as in the former case the storage ring and the detector really 'sees' each other and relative geometric considerations are of much relevance. The observed number of events in a given period of time depends on the choice of the radioactive ion, the boost factor γ and the details of the setup (which include storage ring parameters, detector configuration and the short base-length between them). As alluded to earlier, the maximum γ available is limited by the storage ring configuration. With a view to optimising the setup, we summarise the essential inputs as follows:

- Storage ring parameters: Total length 6880 m, length of a straight section, $S = 2500$ m, number of beta decays in the straight section, $N_0 = 1.1 \times 10^{18}$ per year.
- Detector configuration: The detector material is[5] iron ($\rho = 7.87$ gm/cc). We consider a detector of mass 5 kT. For a given material, this fixes the length of the detector as the radius is changed. It varies from 202.13 m to 12.63 m as the radius ranges over 1m to 4m.
- Base-length: Results are presented for three representative values of the distance of the detector from the storage ring, $L = 200$ m, 500 m, 1 km.
- Boost factor γ: The tau production threshold (3.5 GeV) calls for a high γ. We consider $\gamma = 250, 350, 450$ for ^{8}B and as large as 800 for ^{18}Ne.

The high collimation achievable in the beta-beams encourages the choice of a detector of cylindrical shape coaxial with the storage ring straight section. As γ increases, the RPV event rates increase for the following reasons:

[4]These cross sections include all nuclear effects for an iron target.

[5]Brief comments are made about a water Čerenkov detector in sec. IV.2.

1. an increasingly larger part of the beam falls onto the detector,
2. more neutrinos have enough energy to produce a tau lepton,
3. with the more energetic neutrinos the cross section is larger.

The first two effects are demonstrated by Fig. 5. The geometry integrated flux, Φ, as defined

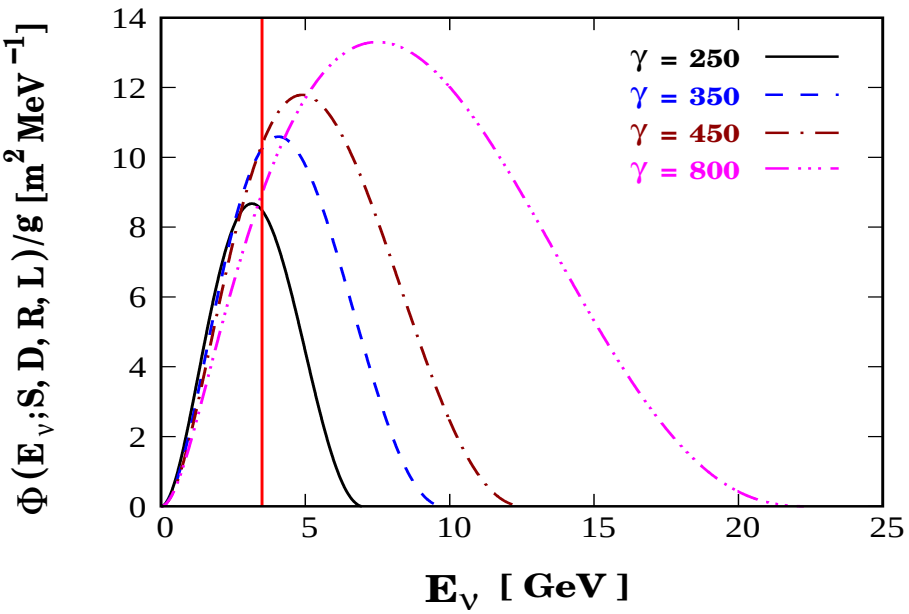

Figure 5: Geometry integrated flux $\Phi(E_\nu; S, D, R, L)/g$ taking ^{8}B as the decaying ion is plotted against neutrino energy E_ν for different γ for $S = 2500$ m, $D = 202.13$ m, $R = 1$ m, and $L = 200$ m. The vertical line at 3.5 GeV indicates the tau production threshold energy.

in eq. 5, represents the beta-beam neutrino flux spectrum falling onto the detector per unit time. It is seen that as γ increases, the total area under the curve also increases, illustrating the first effect. The area under the curves on the right side of the vertical line (the threshold) also increases with γ, in conformity with the second expectation. For a high γ the beam should saturate. However, with the γ used in Fig. 5 this is not evident due to the enormous length of the straight section of the storage ring: To collimate the flux emanating from the rear part of the ring a very high γ will be needed.

As geometry plays a crucial role in optimising the near-detector setup, we study the detector length dependence of the expected number of RPV events for different base-lengths and different γ. We consider the contribution coming from the two options – the $\lambda'\lambda'$ and $\lambda\lambda'$ processes – in different panels for every figure, assuming the RPV coupling constants saturate present experimental upper limits.

IV.1 Choice of ion source and detector

The choice of ^{8}B as the ion source provides the most attractive option due to its high end-point energy. Iron calorimeters are preferred for the smaller size and significant background removal.

To get a glimpse of the number of events one might expect in such a setup, let us present the following estimate. A 5 kT Fe detector of radius 1 m (length 202.13 m) placed at a distance 200 m from the decay ring can give rise to 92 (24) muon events via the $\lambda'\lambda'$ ($\lambda\lambda'$) process in 5 years for[6] $\gamma = 250$.

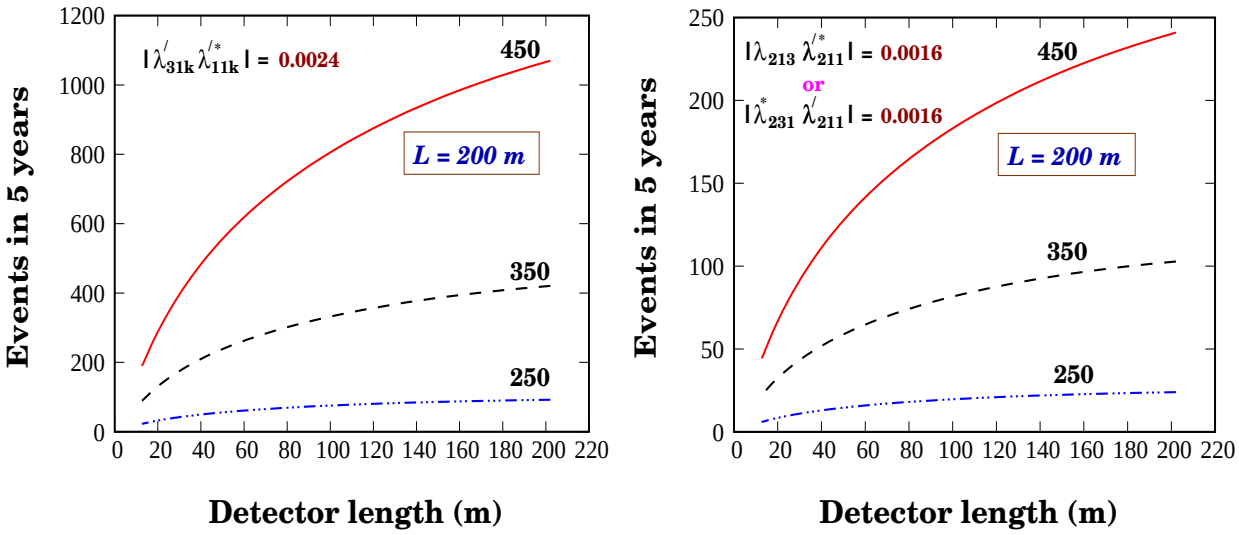

Figure 6: Expected number of RPV muon events in five years for a 5 kT iron detector vs. the detector length for $\gamma = 250$, 350, and 450 for ^{8}B beta-beam flux. The left (right) panel is for the $\lambda'\lambda'$ ($\lambda\lambda'$) driven process. $k = 2, 3$.

In Fig. 6 we exhibit the γ dependence of the expected number of muon events over a five-year period for a fixed base-length of 200 m. Collimation plays a role as is demonstrated by the increase in the number of events for higher γ. As expected, a long detector serves better as it provides more opportunity for a neutrino interaction to occur. However, this increase with the length is not linear; a part of the beam is lost due to the concomitant decrease in the radius (to keep the total mass fixed at 5 kT). In addition, with the increase in detector length as the detector efficiency decreases, the increase in the rates is also somewhat restricted.

It is also of interest to study the base-length dependence of the number of events. The beam spreads with an increase in the base-length, reducing the effective flux hitting the detector. This causes a fall in the number of events (other parameters remaining the same) as shown in Fig. 7. It is interesting to note that the increase in the number of events with increase in

[6]The corresponding numbers for $\gamma = 350$ are 421 (103).

the length of the detector gets severely diluted at larger base-lengths.

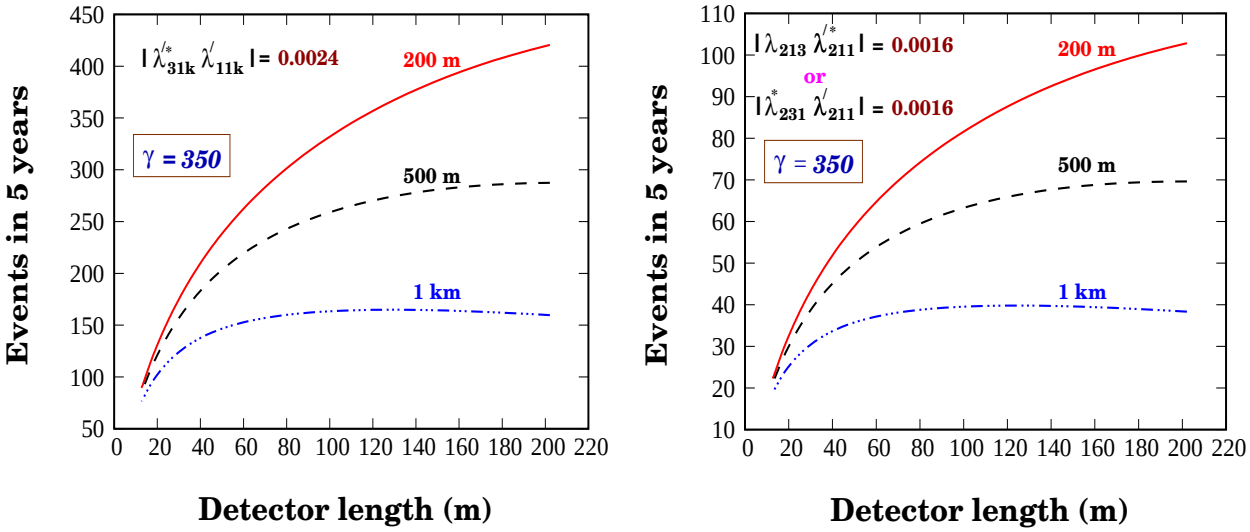

Figure 7: Muon signal event rate in 5 years as a function of the detector (Fe) length for three different choices of base-length have been shown for ^{8}B beta-beam flux. The left (right) panel corresponds to the $\lambda'\lambda'$ ($\lambda\lambda'$) driven process. $k = 2, 3$.

While presenting the expected number of events we assumed the RPV couplings saturate the present experimental upper bounds. In case less or even no events are seen, the existing limits on the combinations $|\lambda'^{\star}_{31k}\lambda'_{11k}|, k = 2, 3$, $|\lambda^{\star}_{231}\lambda'_{211}|$ and $|\lambda_{213}\lambda'^{\star}_{211}|$ will be improved. Choosing the minimum number of non-zero RPV couplings, one can put conservative upper bounds. In Fig. 8 we show the bounds – the region above the curves are disallowed – achievable in the case of 'no-show'[7]. It is seen that to put stringent bounds it is necessary to go for a higher γ and a longer detector.

IV.2 Alternative setups

Although so far we have presented results with ^{8}B as the beta-beam source, ^{18}Ne is the most discussed decaying ion in the literature. As mentioned earlier, due to the smaller end-point energy of ^{18}Ne, a high γ is required to cross the τ threshold. Fig. 9 depicts the variation in the expected event rate with detector length for ^{18}Ne with $\gamma = 800$ using a 5 kT iron calorimeter. We see that due to high γ for ^{18}Ne, the beam is so collimated that the event rates increase almost linearly with increasing detector length in contrast to the ^{8}B case we have presented. However even in such an extreme scenario, where we use the same storage ring configuration to reach such a high γ, the expected event rates are comparable to that in the ^{8}B case. Hence we conclude that ^{8}B is preferred to ^{18}Ne in exploring lepton number

[7] At 95% CL this corresponds to not more than 3 events.

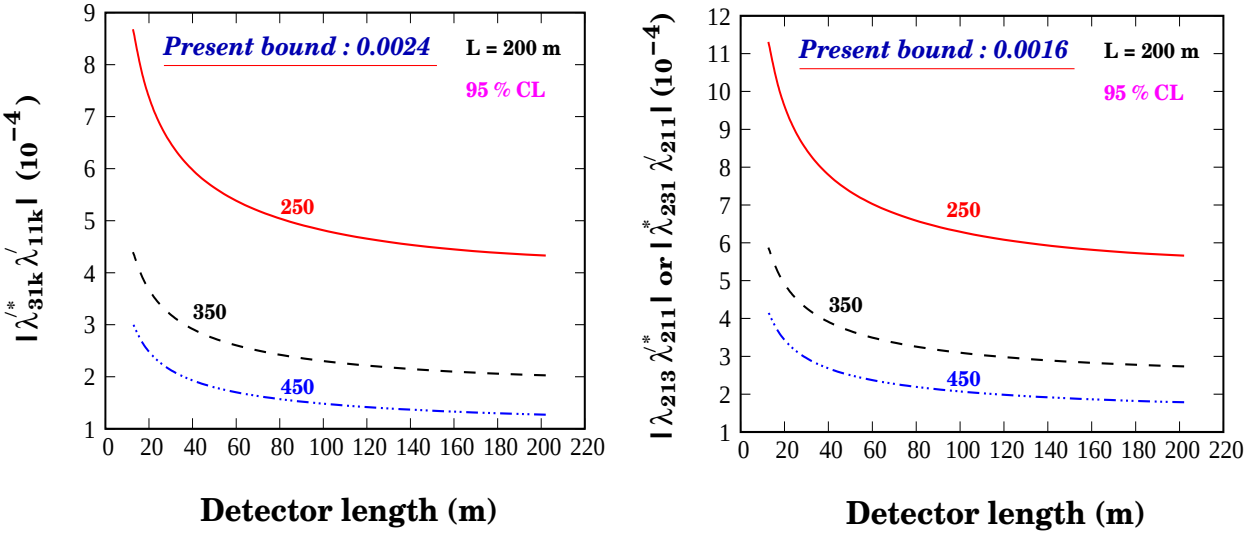

Figure 8: Bounds on $|\lambda'^{\star}_{31k}\lambda'_{11k}|$, $k = 2, 3$ ($|\lambda^{\star}_{231}\lambda'_{211}|$ or $|\lambda_{213}\lambda'^{\star}_{211}|$) versus detector size at 95% CL for zero observed events is depicted in left (right) panel for $\gamma = 250, 350, 450$. The bounds scale as $(\tilde{m}/100\ \text{GeV})^2$. The results are for a five-year run for a 5 kT Fe detector placed at a distance of 200 m from the front end of the storage ring for ^{8}B beta-beam flux.

violating signatures with beta-beams.

The use of water Čerenkov detectors with good capability of muon-electron separation and moderate efficiency of neutral current rejection may be an interesting option to see the signals of new physics and to normalize the incoming flux. The disadvantage of this set-up turns out to be the huge background. Consider a 5 kT water Čerenkov detector with radius 2.5 m at a distance 200 m from the decay ring. In five years, this will lead to 45 (12) muon events from τ-lepton decay for $\lambda'\lambda'$ ($\lambda\lambda'$) driven processes from an incoming ^{8}B ν_e beam accelerated with a γ of 250 and with a muon detection threshold of 200 MeV. For the same configuration and duration, one expects roughly 10^8 pions produced from charged and neutral current interactions of the ν_e beam. Muons produced from π decay will thus completely swamp the signal.

The number of signal events may be increased by designing a very long water detector with small radius though this could be technologically challenging. In any case, the background events will continue to be very high. So, this option also does not hold much promise. The basic problem of high backgrounds, avoided in the Fe detector, will also plague totally active scintillator based detectors.

V Discussion and conclusion

Beta-beam experiments may be sensitive to the lepton number violating interactions. In [5] it was shown that RPV L-violating interactions can interfere with pure oscillation signals in long-baseline beta-beam experiments. In this paper we explore a complementary scenario.

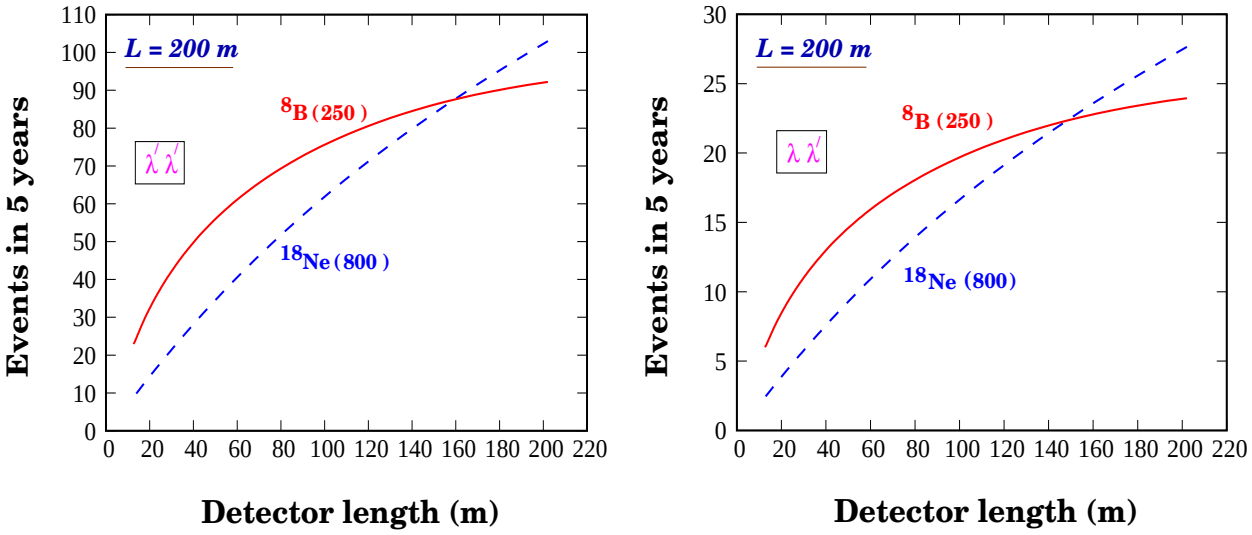

Figure 9: Comparison of the muon signal event rates as a function of the detector length for a 5 kT iron calorimeter placed at a distance of 200 m from the storage ring for $\gamma = 800$ (250) with ^{18}Ne (^{8}B). The left and right panels correspond to $\lambda'\lambda'$ and $\lambda\lambda'$ driven processes, respectively.

We propose that to probe such interactions, an iron calorimeter detector placed close to the storage ring holds promise as it provides essentially a neutrino oscillation free environment. In particular, the combination of a 5 kT cylindrical iron detector placed within a distance of 200 m to 1 km from the decay ring and a neutrino beam from an ^{8}B ion source with γ in the range 250 to 450, running for 5 years is well-suited in this regard. We have examined the impact of non-trivial design details of such a near-detector setup.

At production, low energy β-decay experiments may get contaminated by tau neutrinos through RPV interactions. We show that, this contamination, though small, can be probed using the above setup. RPV interactions can also play a role in such an experiment during the interactions of the beta-beam electron neutrinos with the detector.

It is interesting to explore if RPV interactions can affect beta-beam experiments in other ways. For example, we have checked that the impact of these interactions on the μ detection cross section is insignificant. As mentioned earlier, ν_μ may be produced in beta decay through RPV interactions but this also is severely suppressed as the corresponding couplings have stringent upper limits.

We have presented results for a neutrino beam. Anti-neutrino beams can also be produced using ^{8}Li or ^{6}He as sources. In fact, a storage ring design may allow both beams to be present simultaneously. The expected event rates for anti-neutrinos are of similar order as for the neutrinos.

In conclusion, we find a near-detector setup can be useful for exploring lepton number vi-

olating interactions with beta-beams. It may allow us to put stringent bounds on some of these couplings.

Acknowledgments

SKA is grateful to N.K. Mondal for illuminating discussions. He would like to acknowledge help from S.M. Shalgar and A. Samanta for the GEANT and Nuance based simulation. SR benefitted from discussions with G. Majumder on pion background issues. He would like to thank the Saha Institute of Nuclear Physics, Kolkata, India for a fellowship in the early stages of this work. He also acknowledges support from 'Bundesministerium für Bildung und Forschung', Berlin/Bonn. SKA and AR acknowledge support from a DST, India research project at the University of Calcutta during the initial period.

References

[1] P. Zucchelli, Phys. Lett. B **532** (2002) 166.

[2] M. Mezzetto, J. Phys. G **29** (2003) 1771 [arXiv:hep-ex/0302007].

[3] J. Burguet-Castell, D. Casper, J. J. Gomez-Cadenas, P. Hernandez and F. Sanchez, Nucl. Phys. B **695** (2004) 217 [arXiv:hep-ph/0312068].

[4] See, for example, S. K. Agarwalla, A. Raychaudhuri and A. Samanta, Phys. Lett. B **629** (2005) 33 [arXiv:hep-ph/0505015].

[5] R. Adhikari, S. K. Agarwalla and A. Raychaudhuri, Phys. Lett. B **642** (2006) 111 [arXiv:hep-ph/0608034].

[6] For reviews, see C. Albright *et al.* [Neutrino Factory/Muon Collider Collaboration], arXiv:physics/0411123; P. Huber, M. Lindner, M. Rolinec and W. Winter, Phys. Rev. D **73** (2006) 053002 [arXiv:hep-ph/0506237]; C. Volpe, J. Phys. G **34** (2007) R1 [arXiv:hep-ph/0605033].

[7] C. Volpe, J. Phys. G **30** (2004) L1 [arXiv:hep-ph/0303222].

[8] P. Fayet, Phys. Lett. B **69** (1977) 489; G. R. Farrar and P. Fayet, Phys. Lett. B **76** (1978) 575.

[9] R. Barbier *et al.*, Phys. Rept. **420** (2005) 1 [arXiv:hep-ph/0406039]; M. Chemtob, Prog. Part. Nucl. Phys. **54** (2005) 71 [arXiv:hep-ph/0406029].

[10] J. Bouchez, M. Lindroos and M. Mezzetto, AIP Conf. Proc. **721** (2004) 37 [arXiv:hep-ex/0310059].

[11] J. Burguet-Castell, D. Casper, E. Couce, J. J. Gomez-Cadenas and P. Hernandez, Nucl. Phys. B **725** (2005) 306 [arXiv:hep-ph/0503021].

[12] A. Donini, E. Fernandez, P. Migliozzi, S. Rigolin, L. Scotto Lavina, T. Tabarelli de Fatis and F. Terranova, arXiv:hep-ph/0511134.

[13] M. Lindroos, "Accelerator based neutrino beams", Talk at Moriond meeting, March 2003.

[14] L.P. Ekstrom and R.B. Firestone, WWW Table of Radioactive Isotopes, database version 2/28/99 from URL http://ie.lbl.gov/toi/

[15] C. Rubbia, A. Ferrari, Y. Kadi and V. Vlachoudis, Nucl. Instrum. Meth. A **568** (2006) 475 [arXiv:hep-ph/0602032].

[16] E. Fernandez-Martinez, arXiv:hep-ph/0605101.

[17] B. Autin *et al.*, J. Phys. G **29** (2003) 1785 [arXiv:physics/0306106].

[18] F. Terranova, A. Marotta, P. Migliozzi and M. Spinetti, Eur. Phys. J. C **38** (2004) 69 [arXiv:hep-ph/0405081].

[19] A. Donini and E. Fernandez-Martinez, Phys. Lett. B **641** (2006) 432 [arXiv:hep-ph/0603261].

[20] K. Hagiwara *et al.* [Particle Data Group], Phys. Rev. D **66** (2002) 010001.

[21] A. Donini, E. Fernandez-Martinez, P. Migliozzi, S. Rigolin, L. Scotto Lavina, T. Tabarelli de Fatis and F. Terranova, Eur. Phys. J. C **48** (2006) 787 [arXiv:hep-ph/0604229].

[22] P. Wintz (on behalf of SINDRUM II Collaboration), Proc. of the 14th Intl. Conf. on Particles and Nuclei (PANIC96), (World Scientific 1997, Eds. C. E. Carlson and J. J. Domingo) 458; J. E. Kim, P. Ko and D. G. Lee, Phys. Rev. D **56** (1997) 100 [arXiv:hep-ph/9701381].

[23] GEANT - Detector Description and Simulation Tool CERN Program Library Long Writeup W5013.

[24] D. Casper, Nucl. Phys. Proc. Suppl. **112** (2002) 161 [arXiv:hep-ph/0208030].

[25] J. Serreau and C. Volpe, Phys. Rev. C **70** (2004) 055502 [arXiv:hep-ph/0403293].

[26] Adrian Fabich, private communication.

[27] L. E. Ibáñez and G. G. Ross, Nucl. Phys. B **368** (1992) 3; H. K. Dreiner, C. Luhn and M. Thormeier, Phys. Rev. D **73** (2006) 075007 [arXiv:hep-ph/0512163].

[28] A. Datta, R. Gandhi, B. Mukhopadhyaya and P. Mehta, Phys. Rev. D **64** (2001) 015011 [arXiv:hep-ph/0011375].

[29] P. Huber, T. Schwetz and J. W. F. Valle, Phys. Rev. D **66** (2002) 013006 [arXiv:hep-ph/0202048].

[30] M. Hirsch, H. V. Klapdor-Kleingrothaus and S. G. Kovalenko, Nucl. Phys. Proc. Suppl. **62** (1998) 224.

[31] G. Bhattacharyya, H. V. Klapdor-Kleingrothaus and H. Päs, Phys. Lett. B **463** (1999) 77 [arXiv:hep-ph/9907432].

[32] K. Agashe and M. Graesser, Phys. Rev. D **54** (1996) 4445 [arXiv:hep-ph/9510439].

[33] H. L. Lai *et al.*, Phys. Rev. D **55** (1997) 1280 [arXiv:hep-ph/9606399].

[34] E. A. Paschos, L. Pasquali and J. Y. Yu, Nucl. Phys. B **588** (2000) 263 [arXiv:hep-ph/0005255]; E. A. Paschos and J. Y. Yu, Phys. Rev. D **65** (2002) 033002 [arXiv:hep-ph/0107261].